

The nanogeochemistry of abiotic carbonaceous matter in serpentinites from the Yap Trench, western Pacific Ocean

Jingbo Nan(南景博)^{1,2,5}, Helen E. King², Guusje Delen³, Florian Meirer³, Bert M. Weckhuysen³, Zixiao Guo(郭自晓)^{4,1}, Xiaotong Peng(彭晓彤)^{1*} and Oliver Plümper^{2*}

¹Institute of Deep Sea Science and Engineering, Chinese Academy of Sciences, Sanya 572000, China

²Department of Earth Sciences, Utrecht University, 3584 CD Utrecht, the Netherlands

³Debye Institute for Nanomaterials Science, Utrecht University, 3584 CG Utrecht, the Netherlands

⁴College of Resource and Environmental Sciences, Hebei Normal University, Shijiazhuang 050024, China

⁵University of Chinese Academy of Sciences, Beijing 100049, China

ABSTRACT

Serpentinization may provide a unique environment for the abiotic formation of condensed carbonaceous matter. This could support the deep biosphere and contribute to the deep carbon cycle, and may have provided the first building blocks for life. However, thus far, condensed carbonaceous matter has been found only in association with the minor mineral constituents of serpentinites. In contrast, here we show the direct association between carbonaceous matter and the dominant Fe oxide in serpentinites, magnetite. Our samples were recovered from the Yap Trench, western Pacific Ocean, with a human-occupied vehicle at a depth of 6413 m below sea level. The carbonaceous matter coincides with some micron-sized magnetite grains, but particularly with nanosized Fe oxides within serpentinite nanopores. Vibrational spectroscopy reveals that the condensed carbonaceous matter contains both aliphatic and aromatic compounds, but there is no evidence for functional groups typical for biological organics. Based on these observations, we suggest that physicochemical phenomena in serpentinite nanopores and nanosized catalytically active minerals may play a key role in the abiotic synthesis of complex carbonaceous matter.

INTRODUCTION

Hydrogen production during peridotite serpentinization is thought to form unique geochemical environments that provide energy sources for microbial ecosystems (Ohara et al., 2012). Although it is not always straightforward to discern abiotic from biotic organic matter in natural systems (e.g., Plümper et al., 2017a), evidence suggests that serpentinites have a high potential for the production of organic compounds, such as CH₄, short-chain hydrocarbons, and condensed carbonaceous matter (CCM) (McCollom, 2013).

The close spatial relationship between (1) specific minerals that are used in chemical industries as solid catalysts, and (2) organics highlights the potential of serpentinites for organic synthesis (Andreani and Ménez, 2019, and references therein). For example, Ménez et al. (2018)

reported the occurrence of serpentinite-hosted abiotic amino acids, which they interpreted to have formed via Friedel-Crafts reactions catalyzed by Fe-rich saponite clay. This observation, among others (e.g., Sforza et al., 2018), suggests that complex organics can form abiotically via mineral-based catalysis during serpentinization. Beyond clay minerals, primary chromite grains (Foustoukos and Seyfried, 2004) as well as Fe oxides (e.g., Fe₃O₄; Fu et al., 2007), Ni-Fe alloys (Horita and Berndt, 1999), and Fe-Ni sulfides (Camprubi et al., 2017) produced during serpentinization are thought to exert a first-order control on the abiogenic synthesis of organic matter.

Another commonly overlooked property of serpentinites that may promote organic molecule generation is their extensive nanoscale porosity (10–200 nm; Tutolo et al., 2016). Recent molecular simulations suggest there is an increased thermodynamic drive toward key precursors for hydrocarbon production when CO₂ and H₂ are

confined within inorganic structures (Le et al., 2017). Critically, shifts in equilibrium at the molecular level occur due to adsorption and potential catalysis at the pore walls when a fluid with restricted diffusive transport is present (Cole and Striolo, 2019).

Nano-sized materials are also associated with elevated surface area, providing ample active sites for surface chemical reactions. Thus, if the above-mentioned catalytic minerals are present in the nanosize regime in serpentinites, they may be much more viable producers of organic matter than has previously been shown with free-surface, geometrically unconfined experiments (e.g., Foustoukos and Seyfried, 2004).

Here we use correlative nanoscale imaging and vibrational spectroscopy to probe the nanoscale regime of serpentinites from the Yap Trench, western Pacific Ocean, and demonstrate an intimate association between CCM, magnetite, and serpentine nanoporosity. The nanoscale pore size and the microstructural relationships between the inorganic mineralogy and the organic matter suggest that the CCM is of abiotic origin.

SAMPLES AND ANALYSIS

The rock sample was recovered by the human-occupied vehicle (HOV) *Jiaolong* at 6413 m below sea level at the outer forearc trench wall (see the Supplemental Material¹ for the geological setting). Subsamples were extracted from the internal regions of the original rock sample to avoid contamination. All subsamples were cleaned and subdivided into polished, resin-free rock chips and freshly broken fragments. Subsamples were investigated

*E-mails: xtpeng@idsse.ac.cn; o.plumper@uu.nl

¹Supplemental Material. Methods and supplemental information. Please visit <https://doi.org/10.1130/GEOL.S.13125335> to access the supplemental material, and contact editing@geosociety.org with any questions.

using Raman spectroscopy and focused ion-beam scanning electron microscopy (FIB-SEM). FIB-SEM was also used to excavate seven electron-transparent foils for (scanning) transmission electron microscopy ([S]TEM). Microstructural and chemical data were cross-correlated with molecular information obtained by photo-induced force microscopy (PiFM). Details regarding the sample preparation and analytical methods are provided in the Supplemental Material.

ROCK CHARACTERIZATION

The rock is a serpentinized harzburgite (Fig. S1 in the Supplemental Material) characterized by relics of primary olivine ($X_{Mg} = 0.86$), orthopyroxene, and Cr-spinel. Mesh-textured serpentine (lizardite \pm chrysotile \pm brucite; $X_{Mg} = 0.88 \pm 0.03$), magnetite, and talc, as well as elevated X_{Mg} within mesh-textured serpentine over olivine, suggest that serpentinization occurred at 200–300 °C (Klein et al., 2014). Fe-rich phases occur in two size regimes: micron-sized (<30 μm) magnetite grains with irregular shapes (Figs. 1A and 1B; Fig. S7), and Fe-oxide nanofibers (~50 nm in length; Figs. 1C–1E) that form randomly oriented aggregates. Energy-dispersive X-ray spectroscopy (EDX) mapping

within the TEM, and PiFM analysis (Fig. S5), support the interpretation that the nanofibers are Fe oxides; however, a hydroxide component cannot be excluded. Lack of uniformly shaped spheres or nanocrystals aligned along filamentous organic structures (e.g., Schefel et al., 2006), expected for microbial Fe-(hydr)oxide, indicates that the Fe (hydr)oxides here are abiotic, likely formed after the main serpentinization.

Large patches (10–20 μm) of CCM occur within cavities between olivine, mesh serpentine, and/or magnetite grains (Fig. 1A). At the edges of the patches, disorderly Fe-(hydr)oxide fibers grow out from micron-sized serpentine and magnetite grains, penetrating as much as 50 nm into the CCM (Fig. 1D). CCM is also found within nanometer-sized serpentine pores and are commonly associated with Fe-(hydr)oxide grains that coat the serpentine pore walls (Figs. 1E and 1F; Fig. S4). Nanoporosity (median pore size = 50 nm) is abundant throughout all samples and concentrated within mesh cores (Fig. 2).

CARBON NANOGEOCHEMISTRY

Raman spectra from large patches of CCM (Fig. 3A) show modes corresponding to CH_2

deformation (1300 cm^{-1}) and C-H deformation (1450 cm^{-1}) and a broader region between 2850 and 2960 cm^{-1} (CH_2 stretching at 2850 and 2880 cm^{-1} ; CH_3 stretching at 2960 cm^{-1}) indicating the presence of aliphatic compounds. A weak mode close to the 1600 cm^{-1} region indicates that CCM has an aromatic component. Non-contact mode atomic force microscopy imaging (Fig. 3B) combined with principle component analysis (see the Supplemental Material) of hyperspectral PiFM images (Fig. 3C) confirms that individual nanopores are filled with CCM with a distinct aromatic C = C stretching mode (Fig. 3D). The direct CCM-nanoporosity association is further corroborated by visualizing the aromatic C = C stretching mode at 1492 cm^{-1} across an area of 2.3 μm^2 (Fig. 3E). Here, >70% of the nanoporosity contains CCM.

As a reference, we also prepared a FIB foil in an area of the sample that showed neither macroscopically identifiable organics nor magnetite grains. TEM analysis reveals the ubiquitous presence of nanoporosity, but no CCM was detected with either EDX-STEM mapping or PiFM analysis (Fig. S9).

ORIGIN OF THE CONDENSED CARBONACEOUS MATTER

The CCM has aliphatic and/or aromatic groups and no evidence for functional groups. In contrast, vibrational spectroscopy of microorganisms and extracellular polymeric substances show a variety of different functional groups. Prokaryotic microorganisms are typically a few micrometers large and are thus unlikely to colonize the observed serpentine nanoporosity (Ménez et al., 2018). Vibrational modes characteristic for thermal degradation of biogenic organic matter, i.e., graphitic carbon (e.g., Dodd et al., 2019), are also absent. A lack of functional groups is consistent with suggested abiotic CCM in serpentinites from the Ligurian Tethyan ophiolites (Sforna et al., 2018). It is also expected that any externally derived C-O-H fluids that could carry hydrocarbons would result in homogeneously distributed organics within pore spaces rather than the specific association to Fe oxides observed here. Hence, based on molecular and microstructural evidence, we suggest that the CCM identified here is of abiotic origin.

The direct association of CCM with Fe oxides suggests that organic synthesis may have occurred via a Fischer-Tropsch-type mechanism, likely constraining the temperature conditions to <200 °C (McCullom, 2013), concomitant with the inferred serpentinization conditions (200–300 °C). Future investigations will need to determine the formation conditions and catalytic activity of nanoscale Fe oxides (Fig. 1). Even if the Fe minerals are hydroxylated, nanoscale Fe (hydr)oxides may have different catalytic activities compared to their macroscopic counterparts.

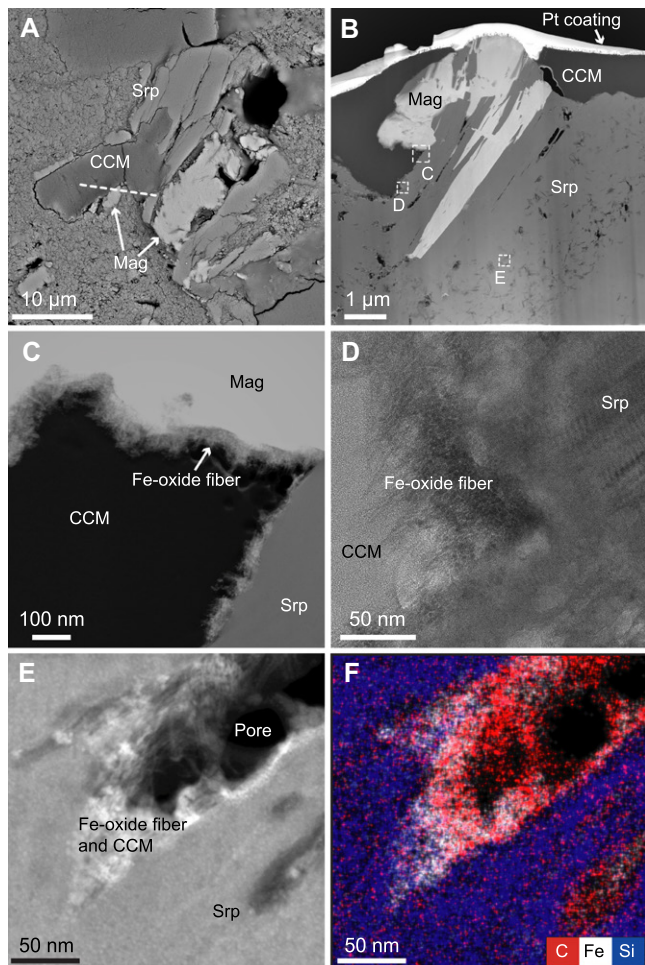


Figure 1. Spatial association of carbonaceous matter with Fe oxides and serpentine nanoporosity. (A) Back-scattered electron image of microscale condensed carbonaceous matter (CCM) and its association with magnetite (Mag; dashed line is focused ion beam foil location). (B) High-angle annular dark-field-scanning transmission electron microscopy image showing location of CCM along the serpentine (Srp)-magnetite interfaces. Pt—platinum. (C) Enlarged view of area shown in B. (D) Transmission electron microscopy (TEM) image showing Fe-oxide nanofibers at the CCM-serpentine interface shown in B. (E,F) Enlarged view of area shown in B (E) and corresponding energy-dispersive X-ray spectroscopy (EDX) maps for carbon (red), iron (white), and silicon (blue) (F).

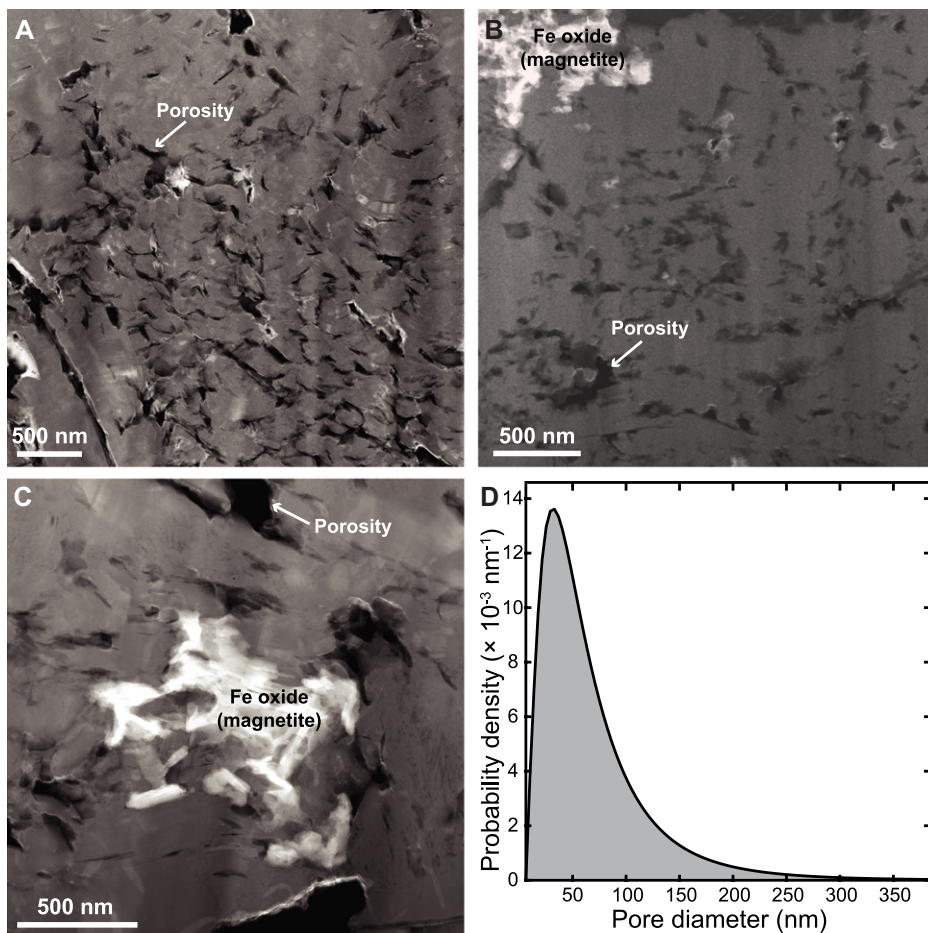


Figure 2. Nanoporosity within Yap Trench (western Pacific Ocean) serpentinites. (A–C) High-angle annular dark-field–scanning transmission electron microscopy images showing morphology and distribution of pore space within serpentine mesh cores. Pore walls are commonly coated with Fe oxides as shown in Figure 1E. Fe-oxide aggregates are scattered throughout the mesh core as depicted in C. (D) Probability density of pore diameter in serpentine mesh cores ($N = 466$ pores).

Fluids released from the subducting slab are a likely carbon source for driving abiotic synthesis of CCM within forearc-derived serpentinites. A first estimation indicates that $280 \text{ mol CO}_2/\text{m}^3$ rock are required to generate CCM, assuming 10% of the nanoporosity is catalytically active (see the Supplemental Material). Although we are lacking key parameters to determine the catalytic activity of serpentinites, the aforementioned CO_2 amount is marginal compared to recent observations suggesting that as much as $1.3 \times 10^{10} \text{ mol/yr}$ could be released from slabs into the forearc (Barry et al., 2019). Transport of CO_2 -bearing fluids would be dominated by fracture flow; however, a chemical exchange between fractures and the nanoporous rock matrix would be aided by electrokinetic transport phenomena (Plümper et al., 2017b) facilitating a continuous renewal of fluids even in dead-end pore systems (Kar et al., 2015). The chemical exchange across fracture walls into nanoporous serpentinites has already been suggested to aid CH_4 synthesis (Le et al., 2017), but exact mechanisms have yet to be investigated.

Similarly, organic molecule synthesis and CCM formation, enabled by the low aqueous solubility of organic molecules (Kamlet et al., 1987), should result in chemical gradients encouraging CO_2 to enter the pores.

NANOSCALE EFFECTS ON ABIOTIC SYNTHESIS

A potential missing link between the abiotic synthesis in natural subsurface systems and the inconsistent observations of Fe-oxide, particularly magnetite, catalysis in experiments (McCullom, 2013) could be the physical effects associated with the ubiquitous presence of nanoporosity. As highlighted above, the Yap Trench samples show a direct association between CCM and nanoporosity, suggesting that nanoscale effects are potentially significant. Previous studies have shown that nanoporosity is ubiquitous in serpentinites (Tutolo et al., 2016) and could potentially account for as much as 90% of the total mineral surface area in any rock (Wang et al., 2003). Decreasing Fe-oxide grain size to the nanoscale (Fig. 2; Fig. S4) should enhance

catalytic activity due to a substantial increase in surface area (e.g., Pour et al., 2010). An estimate based on the TEM images (Fig. 1D) suggests that the Fe-(hydr)oxide nanofibers observed here contribute to a twofold increase in surface area compared to a single magnetite crystal occupying the same volume.

Geometric confinement in nanopores has the potential to reduce the activation energy of various chemical reactions (Santiso et al., 2005), which in turn would increase the reaction rate and enhance reaction yields (Derouane et al., 1988; Turner et al., 2002). Recent studies indeed suggest that confinement of fluids within natural nanopores leads to physicochemical processes that substantially deviate from those occurring in microporous systems (e.g., Plümper et al., 2017b; Cole and Striolo, 2019). Molecular simulations also indicate that nanopores promote the partial reduction of CO_2 to CO (Le et al., 2019). Because the mixture of CO and H_2 is the feedstock for organic synthesis via Fischer-Tropsch-type (FTT) reactions, rather than the more naturally abundant CO_2 , this would enhance the catalytic potential of serpentinizing systems.

An increase in CO within the nanoporosity (Cole and Striolo, 2019) may also aid CCM precipitation. Experiments show that CO present during FTT synthesis promotes C-C bond formation, aiding condensed hydrocarbon growth (Weststrate et al., 2020). Thus, CO in nanopores not only may be crucial during initial synthesis stages, but also may play a vital role during CCM precipitation. Catalytic cracking of potentially produced CH_4 may also yield carbonaceous matter (Amin et al., 2011). Moreover, confinement in nanopores may dramatically increase the local CO and CO_2 solubility (e.g., Cole and Striolo, 2019) and as such may increase the local C/ H_2 ratio, supporting aromatic molecule synthesis (Zolotov and Shock, 2000). In turn, a lower C/ H_2 ratio within larger pores could promote the synthesis of aliphatic compounds, explaining the differences in the here-observed CCM compositions.

CONCLUSIONS AND OUTLOOK

We have combined correlative micro- and nanostructural imaging with (nanoscale) vibrational spectroscopy to investigate carbonaceous matter within serpentinites from the Yap Trench. Our results suggest that the organics are of abiotic origin, and, as such, the serpentinites studied here represent some of the first potential evidence for abiotic organic carbon at a subduction-zone trench. Based on our observations, we suggest that geometric confinement and nanostructured, catalytically active metal oxides may play an essential role in the abiotic formation of organics during serpentinization. In conclusion, geochemical processes in nanoporous media, such as serpentinites,

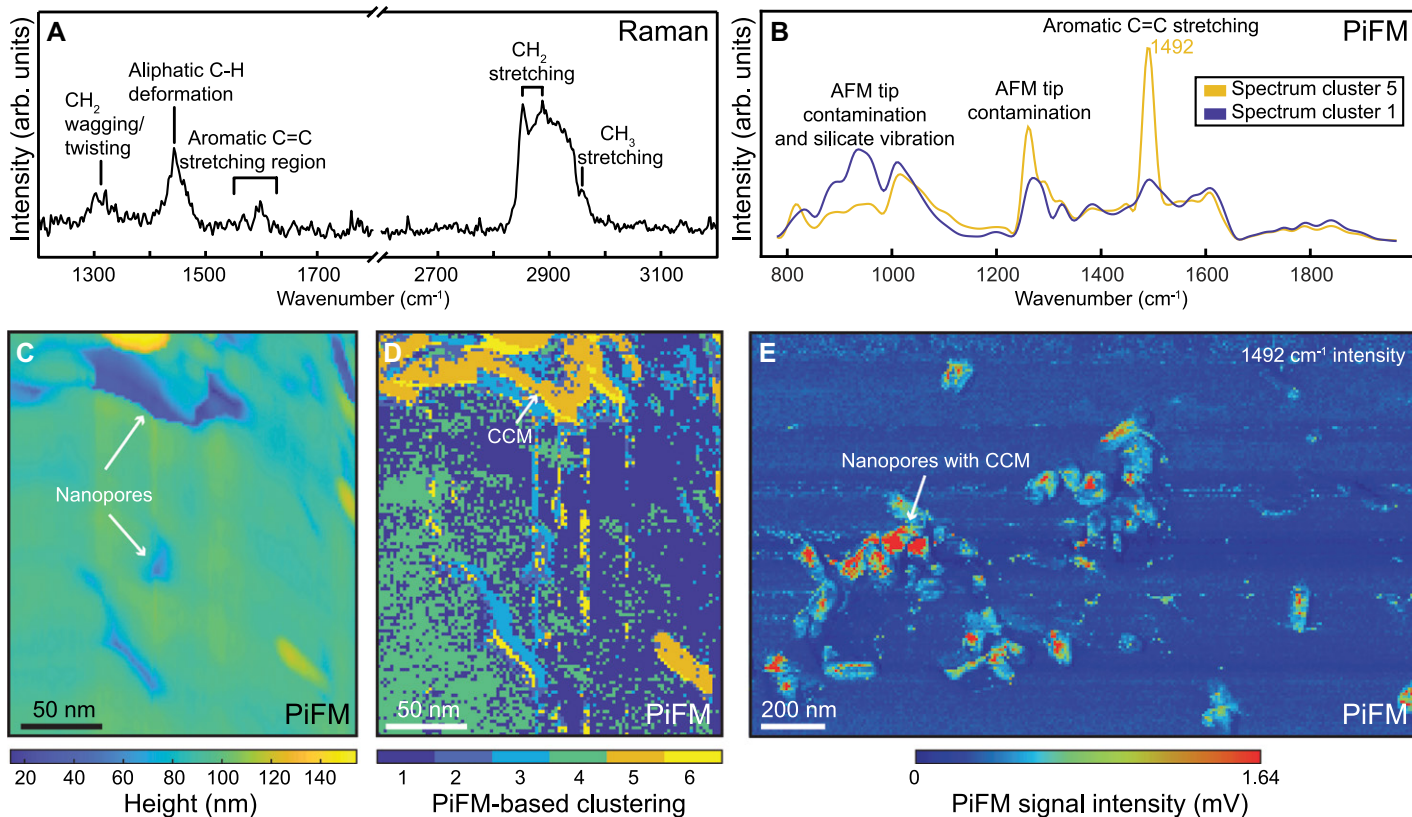


Figure 3. Presence of micron- and nanosized organic compounds within serpentinite. (A) Raman spectrum obtained from micron-sized condensed carbonaceous matter (CCM) shown in Figure 2A. arb.—arbitrary. (B) Average photo-induced force microscopy (PiFM) spectrum corresponding to mineral matrix (cluster 1) and CCM within nanopores (cluster 5; see the Supplemental Material [see footnote 1] for details). AFM—atomic force microscopy. (C) PiFM topographic image of focused ion beam foil showing serpentine nanoporosity. (D) Cluster map of the same area as in C, derived from hyperspectral PiFM image acquired between 760 cm^{-1} and 1860 cm^{-1} . (E) PiFM map at 1492 cm^{-1} across the larger area highlighting widespread abundance of CCM within nanopores.

are largely unexplored despite their potential to support deep-seated biological ecosystems (Ménez et al., 2018) and to generate the first building blocks for the origin of life (Russell et al., 2010).

Based on our findings, future studies on abiotic organic synthesis mimicking natural hydrothermal systems need to focus on the combined efficiency of catalytically active, nanocrystalline minerals and nanoconfinement effects. It will be critical to determine how confinement affects physical properties of geo-fluids and evaluate the surface chemistry of pore walls. Magnetite surfaces in the chemical industry react with gaseous carbon oxide (e.g., CO) and are subsequently converted into Fe metal and/or Fe carbides (e.g., de Smit and Weckhuysen, 2008). However, these phases have never been documented in natural systems. With atomic-resolved chemical imaging via aberration-corrected TEM (Livi et al., 2013) and atom probe tomography (Saxey et al., 2018), it may be possible to identify these surface catalytic sites. Moreover, as in situ liquid and/or gas-cell TEM (Li et al., 2015) and X-ray microscopy (Meirer and Weckhuysen, 2018) become readily available, it may also be possible to directly observe min-

eral-based catalysis at the nanoscale. These analytical and experimental tools will allow us to obtain unprecedented new knowledge about the physicochemical mechanisms operating during serpentinization-driven catalysis.

ACKNOWLEDGMENTS

We thank the crews and scientists aboard R/V *Xiangyanghong 09* and HOV *Jiaolong*. We thank E. Camprubi and P. de Peinder, as well as two anonymous reviewers and Ben Tutolo for constructive criticism. Nan was supported by the China Scholarship Council (CSC) and Plümpner by European Research Council (ERC) starting grant “nano-EARTH” (852069). Funding was also provided by China’s National Key R&D Programmes (NKPs) (grant 2016YFC0304900, 2018YFC0309802, 2017YFC0306702, 2016YFC0300503). Weckhuysen acknowledges the Dutch Research Council (NWO) in the form of a Gravitation program and the ARC CBBC.

REFERENCES CITED

Amin, A.M., Croiset, E., and Epling, W., 2011, Review of methane catalytic cracking for hydrogen production: *International Journal of Hydrogen Energy*, v. 36, p. 2904–2935, <https://doi.org/10.1016/j.ijhydene.2010.11.035>.
 Andreani, M., and Ménez, B., 2019, New perspectives on abiotic organic synthesis and processing during hydrothermal alteration of the oceanic lithosphere, *in* Orcutt, B.N., et al., eds., *Deep*

Carbon: Past to Present: Cambridge, UK, Cambridge University Press, p. 447–479, <https://doi.org/10.1017/9781108677950.015>.

Barry, P.H., et al., 2019, Forearc carbon sink reduces long-term volatile recycling into the mantle: *Nature*, v. 568, p. 487–492, <https://doi.org/10.1038/s41586-019-1131-5>.

Camprubi, E., Jordan, S.F., Vasiliadou, R., and Lane, N., 2017, Iron catalysis at the origin of life: *IUBMB Life*, v. 69, p. 373–381, <https://doi.org/10.1002/iub.1632>.

Cole, D., and Striolo, A., 2019, The influence of nanoporosity on the behavior of carbon-bearing fluids, *in* Orcutt, B.N., et al., eds., *Deep Carbon: Past to Present*: Cambridge, UK, Cambridge University Press, p. 358–387, <https://doi.org/10.1017/9781108677950.012>.

de Smit, E., and Weckhuysen, B.M., 2008, The renaissance of iron-based Fischer-Tropsch synthesis: On the multifaceted catalyst deactivation behavior: *Chemical Society Reviews*, v. 37, p. 2758–2781, <https://doi.org/10.1039/b805427d>.

Derouane, E.G., Andre, J.M., and Lucas, A.A., 1988, Surface curvature effects in physisorption and catalysis by microporous solids and molecular sieves: *Journal of Catalysis*, v. 110, p. 58–73, [https://doi.org/10.1016/0021-9517\(88\)90297-7](https://doi.org/10.1016/0021-9517(88)90297-7).

Dodd, M.S., Papineau, D., She, Z.B., Manikymba, C., Wan, Y.S., O’Neil, J., Karhu, J.A., Rizo, H., and Pirajno, F., 2019, Widespread occurrences of variably crystalline ^{13}C -depleted graphitic carbon in banded iron formations: *Earth and Planetary Science Letters*, v. 512, p. 163–174, <https://doi.org/10.1016/j.epsl.2019.01.054>.

- Foustoukos, D.I., and Seyfried, W.E., 2004, Hydrocarbons in hydrothermal vent fluids: The role of chromium-bearing catalysts: *Science*, v. 304, p. 1002–1005, <https://doi.org/10.1126/science.1096033>.
- Fu, Q., Lollar, B.S., Horita, J., Lacrampe-Couloume, G., and Seyfried, W.E., Jr., 2007, Abiotic formation of hydrocarbons under hydrothermal conditions: Constraints from chemical and isotope data: *Geochimica et Cosmochimica Acta*, v. 71, p. 1982–1998, <https://doi.org/10.1016/j.gca.2007.01.022>.
- Horita, J., and Berndt, M.E., 1999, Abiogenic methane formation and isotopic fractionation under hydrothermal conditions: *Science*, v. 285, p. 1055–1057, <https://doi.org/10.1126/science.285.5430.1055>.
- Kamlet, M.J., Doherty, R.M., Abraham, M.H., Carr, P.W., Doherty, R.F., and Taft, R.W., 1987, Linear solvation energy relationships: 41. Important differences between aqueous solubility relationships for aliphatic and aromatic solutes: *Journal of Physical Chemistry*, v. 91, p. 1996–2004, <https://doi.org/10.1021/j100291a062>.
- Kar, A., Chiang, T.Y., Ortiz Rivera, I., Sen, A., and Velegol, D., 2015, Enhanced transport into and out of dead-end pores: *ACS Nano*, v. 9, p. 746–753, <https://doi.org/10.1021/nn506216b>.
- Klein, F., Bach, W., Humphris, S.E., Kahl, W.-A., Jöns, N., Moskowicz, B., and Berquó, T.S., 2014, Magnetite in seafloor serpentinite—Some like it hot: *Geology*, v. 42, p. 135–138, <https://doi.org/10.1130/G35068.1>.
- Le, T., Striolo, A., Turner, C.H., and Cole, D.R., 2017, Confinement effects on carbon dioxide methanation: A novel mechanism for abiotic methane formation: *Scientific Reports*, v. 7, 9021, <https://doi.org/10.1038/s41598-017-09445-1>.
- Le, T.T.B., Striolo, A., and Cole, D.R., 2019, Partial CO₂ reduction in amorphous cylindrical silica nanopores studied with reactive molecular dynamics simulations: *The Journal of Physical Chemistry C*, v. 123, p. 26,358–26,369, <https://doi.org/10.1021/acs.jpcc.9b07344>.
- Li, Y., Zakharov, D., Zhao, S., Tappero, R., Jung, U., Elsen, A., Baumann, P., Nuzzo, R.G., Stach, E.A., and Frenkel, A.I., 2015, Complex structural dynamics of nanocatalysts revealed in *Operando* conditions by correlated imaging and spectroscopy probes: *Nature Communications*, v. 6, 7583, <https://doi.org/10.1038/ncomms8583>.
- Livi, K.J.T., Schaffer, B., Azzolini, D., Seabourne, C.R., Hardcastle, T.P., Scott, A.J., Hazen, R.M., Erlebacher, J.D., Brydson, R., and Sverjensky, D.A., 2013, Atomic-scale surface roughness of rutile and implications for organic molecule adsorption: *Langmuir*, v. 29, p. 6876–6883, <https://doi.org/10.1021/la4005328>.
- McCullom, T.M., 2013, Laboratory simulations of abiotic hydrocarbon formation in Earth's deep subsurface: *Reviews in Mineralogy and Geochemistry*, v. 75, p. 467–494, <https://doi.org/10.2138/rmg.2013.75.15>.
- Meirer, F., and Weckhuysen, B.M., 2018, Spatial and temporal exploration of heterogeneous catalysts with synchrotron radiation: *Nature Reviews: Materials*, v. 3, p. 324–340, <https://doi.org/10.1038/s41578-018-0044-5>.
- Ménez, B., Pisapia, C., Andreani, M., Jamme, F., Vanbellingen, Q.P., Brunelle, A., Richard, L., Dumas, P., and Réfrégiers, M., 2018, Abiotic synthesis of amino acids in the recesses of the oceanic lithosphere: *Nature*, v. 564, p. 59–63, <https://doi.org/10.1038/s41586-018-0684-z>.
- Ohara, Y., et al., 2012, A serpentinite-hosted ecosystem in the Southern Mariana Forearc: *Proceedings of the National Academy of Sciences of the United States of America*, v. 109, p. 2831–2835, <https://doi.org/10.1073/pnas.1112005109>.
- Plümper, O., King, H.E., Geisler, T., Liu, Y., Pabst, S., Savov, I.P., Rost, D., and Zack, T., 2017a, Subduction zone forearc serpentinites as incubators for deep microbial life: *Proceedings of the National Academy of Sciences of the United States of America*, v. 114, p. 4324–4329, <https://doi.org/10.1073/pnas.1612147114>.
- Plümper, O., Botan, A., Los, C., Liu, Y., Malthes-Sørensen, A., and Jamtveit, B., 2017b, Fluid-driven metamorphism of the continental crust governed by nanoscale fluid flow: *Nature Geoscience*, v. 10, p. 685–690, <https://doi.org/10.1038/ngeo3009>.
- Pour, A.N., Housaindokht, M.R., Tayyari, S.F., and Zarkesh, J., 2010, Fischer-Tropsch synthesis by nano-structured iron catalyst: *Journal of Natural Gas Chemistry*, v. 19, p. 284–292, [https://doi.org/10.1016/S1003-9953\(09\)60059-1](https://doi.org/10.1016/S1003-9953(09)60059-1).
- Russell, M.J., Hall, A.J., and Martin, W., 2010, Serpentinization as a source of energy at the origin of life: *Geobiology*, v. 8, p. 355–371, <https://doi.org/10.1111/j.1472-4669.2010.00249.x>.
- Santiso, E.E., George, A.M., Sliwinski-Bartkowiak, M., and Nardelli, M.B., 2005, Effect of confinement on chemical reactions: *Adsorption*, v. 11, p. 349–354, <https://doi.org/10.1007/s10450-005-5949-9>.
- Saxey, D.W., Moser, D.E., Piazolo, S., Reddy, S.M., and Valley, J.W., 2018, Atomic worlds: Current state and future of atom probe tomography in geoscience: *Scripta Materialia*, v. 148, p. 115–121, <https://doi.org/10.1016/j.scriptamat.2017.11.014>.
- Scheffel, A., Gruska, M., Faivre, D., Linaroudis, A., Plitzko, J.M., and Schüler, D., 2006, An acidic protein aligns magnetosomes along a filamentous structure in magnetotactic bacteria: *Nature*, v. 440, p. 110–114, <https://doi.org/10.1038/nature04382>.
- Sforna, M.C., Brunelli, D., Pisapia, C., Pasini, V., Malferri, D., and Ménez, B., 2018, Abiotic formation of condensed carbonaceous matter in the hydrating oceanic crust: *Nature Communications*, v. 9, 5049, <https://doi.org/10.1038/s41467-018-07385-6>.
- Turner, C.H., Brennan, J.K., Johnson, J.K., and Gubbins, K.E., 2002, Effect of confinement by porous materials on chemical reaction kinetics: *The Journal of Chemical Physics*, v. 116, p. 2138–2148, <https://doi.org/10.1063/1.1431590>.
- Tutolo, B.M., Mildner, D.F., Gagnon, C.V., Saar, M.O., and Seyfried, W.E., Jr., 2016, Nanoscale constraints on porosity generation and fluid flow during serpentinization: *Geology*, v. 44, p. 103–106, <https://doi.org/10.1130/G37349.1>.
- Wang, Y.F., Bryan, C., Xu, H.F., and Gao, H.Z., 2003, Nanogeochemistry: Geochemical reactions and mass transfers in nanopores: *Geology*, v. 31, p. 387–390, [https://doi.org/10.1130/0091-7613\(2003\)031<0387:NGRAMT>2.0.CO;2](https://doi.org/10.1130/0091-7613(2003)031<0387:NGRAMT>2.0.CO;2).
- Weststrate, C.J., Sharma, D., Rodriguez, D.G., Gleeson, M.A., Fredriksson, H.O.A., and Niemantsverdriet, J.W., 2020, Mechanistic insight into carbon-carbon bond formation on cobalt under simulated Fischer-Tropsch synthesis conditions: *Nature Communications*, v. 11, 750, <https://doi.org/10.1038/s41467-020-14613-5>.
- Zolotov, M.Y., and Shock, E.L., 2000, A thermodynamic assessment of the potential synthesis of condensed hydrocarbons during cooling and dilution of volcanic gases: *Journal of Geophysical Research*, v. 105, p. 539–559, <https://doi.org/10.1029/1999JB900369>.

Printed in USA